

Equilibrium and dynamic adsorption isotherms of water vapor on silica gels

Leni L. Quirit* and Elma C. Llaguno

Natural Sciences Research Institute & Institute of Chemistry

University of the Philippines

Diliman, Quezon City

Metro Manila 1001, PHILIPPINES

Static adsorption isotherms of water vapor on five silica gel samples were obtained using saturated salt solutions in a closed isothermal environment. The results were compared to dynamic isotherms generated by a fabricated set-up utilizing flowing streams of wet and dry air mixtures. Mathematical modeling of the isotherms data was used to calculate adsorbent surface characteristics and thermodynamic parameters. Conclusions based on isotherm shapes, possible pore sizes, energies of adsorption and heats of adsorption were comparable for the dynamic and static results. Surface areas however, differed by a dynamic to static factor of 1.3 to 2.0 for three silica gel samples. The surface areas from the water vapor static isotherms were within literature values of the range of surface areas from static nitrogen gas isotherms of commercial silica gels.

Keywords: silica gel; water vapor adsorption isotherms; surface areas; heats and energies of adsorption

INTRODUCTION

Atoms in solids occupy fixed positions due to predominantly coulombic forces of attraction among neighboring atoms. Surface atoms, however, have fewer neighbors compared to atoms beneath them and exhibit from an electrical force imbalance. Adsorption of surrounding gas molecules on to the solid surface atoms compensates for this imbalance.

Reliable adsorption equilibrium data, generally in the form of adsorption isotherms, are important as basis for adsorption process design [1]. Equilibrium methods are fairly accurate but take a considerable amount of time. Dynamic methods are faster but are more susceptible to heat and mass transfer effects. Hence, the range of application and reliability of dynamic results have to be investigated.

Adsorption isotherms of water vapor on various silica gel samples were obtained by a static method and compared with isotherms generated by a fabricated dynamic setup. The static set-up was designed to keep the system undisturbed until

equilibrium was reached. The fabricated dynamic setup was a modified and smaller scale version of the dynamic setup used by Park and Knaebel [3]. Mathematical modeling of the data was done to compare static and dynamic calculated surface characteristics and thermodynamic parameters.

The objective for fabrication of and static comparison with the dynamic setup was to see how accurately the dynamic setup can determine adsorption isotherms at a much shorter time. The study of the water vapor adsorption process provides useful information about solids such as silica gel for separation, desiccation, pollution control, gases purification, and energy transport [1]. Moisture sorption isotherms are also largely the basis for analysis of processes affecting food stability [2]. Unlike silica gel, food is more complex and perishable; hence time duration of moisture sorption isotherm determination is critical. This study uses silica gel as an easier material to handle but has the long range objective of using the fabricated dynamic setup for more complex materials such as food.

*To whom correspondence should be addressed.

MATERIALS AND METHODS

Silica gel samples. Adsorption isotherms of two commercial silica gel samples, two gels prepared by Industrial Technology Development Institute (ITDI) of the Department of Science and Technology (DOST) and a silica gel prepared from rice hull were determined. The silica gel samples are described in Table 1.

Static adsorption isotherm. Around 100 mL of saturated salt solutions (NaOH, KOH, LiCl, KOAc, MgCl₂, K₂CO₃, NaBr, SrCl₂, NaCl, KCl, BaCl₂, and K₂SO₄) were each placed in a glass cylinder (or a plastic cylinder if the saturated salt solution is basic) under the ceramic perforated plate of a 200-mm glass desiccator. In each desiccator, three to five 25-mm diameter glass weighing bottles (each containing around 1 g oven dried—or equilibrated previously from a lower RH environment—and previously weighed silica gel sample) were equilibrated for four days in an incubator (Mettler BE 500) at 30°C and re-weighed. A continuous reading thermohygrometer (testo 608-H1) was placed in each desiccator. The thermohygrometer readings indicated the progress of the adsorption process and the attainment of equilibrium.

Dynamic adsorption isotherm. Dry air was obtained from a compressed air cylinder and divided into two streams of dry air and wet air (produced by passing one stream through a fritted impinger containing ultrapure water and immersed in a circulating bath kept at 30°C). The two streams were mixed in different proportions using valves and flowmeters. The dry air (which was cold, due to expansion from the pressurized cylinder) was warmed prior to mixing with the wet air (to prevent condensation) by passing the dry air through a glass coil which is immersed in the water bath. The mixed air was then passed through a silica gel sample tube situated within a condenser tube (through which water from the 30°C circulating water bath passed). A thermohygrometer (testo 605-H1) at the exit end of the condenser tube was used to detect the RH (relative humidity) and temperature of the air that passed through the sample. A diagram of the setup is shown in Fig. 1.

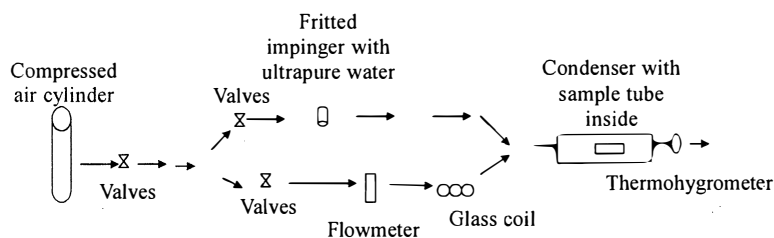


Fig. 1. Active adsorption isotherm set-up (arrows indicate air flow).

It was found that the flow rate at the exit of the air mixture (leading to the hygrometer) was turbulent (as seen when the exit tubing was connected to a flowmeter) when no sample tube was attached to the exit tubing. With a sample tube (containing around 1 g of sample), the flow rate was stable. Equilibration was assumed attained when RH and temperature stabilized after around 1 h of adsorption.

RESULTS AND DISCUSSION

Comparison of hygrometer readings with literature values. Relative humidity (RH) values of saturated salt solutions are cited in the literature for a standard temperature of 25°C. Since tropical conditions made it difficult to maintain this temperature, the incubator was set at 30°C. Published empirical constants [5] were used to calculate RH's at 30°C from the 25°C literature values. The results (and the equation used), are given in Table 2, together with the hygrometer readings of the equilibrated salt solutions.

Only eight out of the 12 saturated salt solutions had available literature constants for RH calculation at 30°C. Of these, saturated solutions of KOH, MgCl₂, NaBr, and SrCl₂ had differences (between calculated and experimental RH values) comparable to experimental RH uncertainties of 0.1–0.2 units. Differences larger than experimental uncertainties were found for the saturated solutions of NaOH, LiCl, and NaCl, ranging

Table 1. Silica gel samples

| Sample | Source | Description |
|------------|---------------------------------------|--|
| Blue Merck | E. Merck Darmstadt, Germany | Commercial silica gel granules with moisture indicator (blue gel) for drying |
| FNG-A | Meigao Chemical Co. Qingdao, China | Commercial white opaque spherical silica gel |
| ITDI II | ITDI Bicutan, MM., Philippines | Glassy granules prepared using 16% SiO ₂ sodium silicate solution 5 N H ₂ SO ₄ , 15% acid excess (4) |
| ITDI III | ITDI Bicutan, MM, Philippines | Glassy granules prepared using 18% SiO ₂ sodium silicate solution 4 N H ₂ SO ₄ , 30% acid excess (4) |
| RHSG 2 | prepared by authors | Translucent silica gel granules prepared from rice hull |

Table 2. Comparison of experimental and literature RH values

| Salt | T Range °C | RH (%) 25°C | A* | B* | Calculated RH 30°C | Experimental RH** 30°C |
|--------------------------------|---------------|----------------|-------|------|-----------------------|---------------------------|
| NaOH | 15–60 | 6 | 5.48 | 27 | 6.0 | 7.3 ± 0.1 |
| KOH | 5–30 | 9 | 0.014 | 1924 | 8.0 | 7.8 ± 0.1 |
| LiCl | 20–65 | 11 | 14.53 | -75 | 11.3 | 12.0 ± 0.2 |
| LiCl | " | " | " | " | " | 12.8 ± 0.1 |
| KOAc | | 22.6 | | | | 22.8 ± 0.2 |
| MgCl ₂ | 5–45 | 33 | 29.26 | 34 | 32.7 | 32.5 ± 0.1 |
| K ₂ CO ₃ | | 43.8 | | | | 43.7 ± 0.2 |
| NaBr | 0–35 | 58 | 20.49 | 308 | 56.6 | 56.5 ± 0.1 |
| SrCl ₂ | 5–30 | 71 | 31.58 | 241 | 70.0 | 70.3 ± 0.1 |
| NaCl | 10–40 | 75 | 69.2 | 25 | 75.2 | 76.4 ± 0.3 |
| KCl | 5–25 | 84 | 49.38 | 159 | | 84.3 ± 0.1 |
| BaCl ₂ | 5–25 | 90 | 69.99 | 75 | | 92.4 ± 2.4 |
| K ₂ SO ₄ | 10–50 | 97 | 86.75 | 34 | 97.1 | Beyond hygrometer range |

*A and B are constants for calculating RH changes with temperature T according to the equation (4):

$RH = A \exp(B/T)$; **Hygrometer readings of equilibrated salt solutions in desiccators inside the incubator

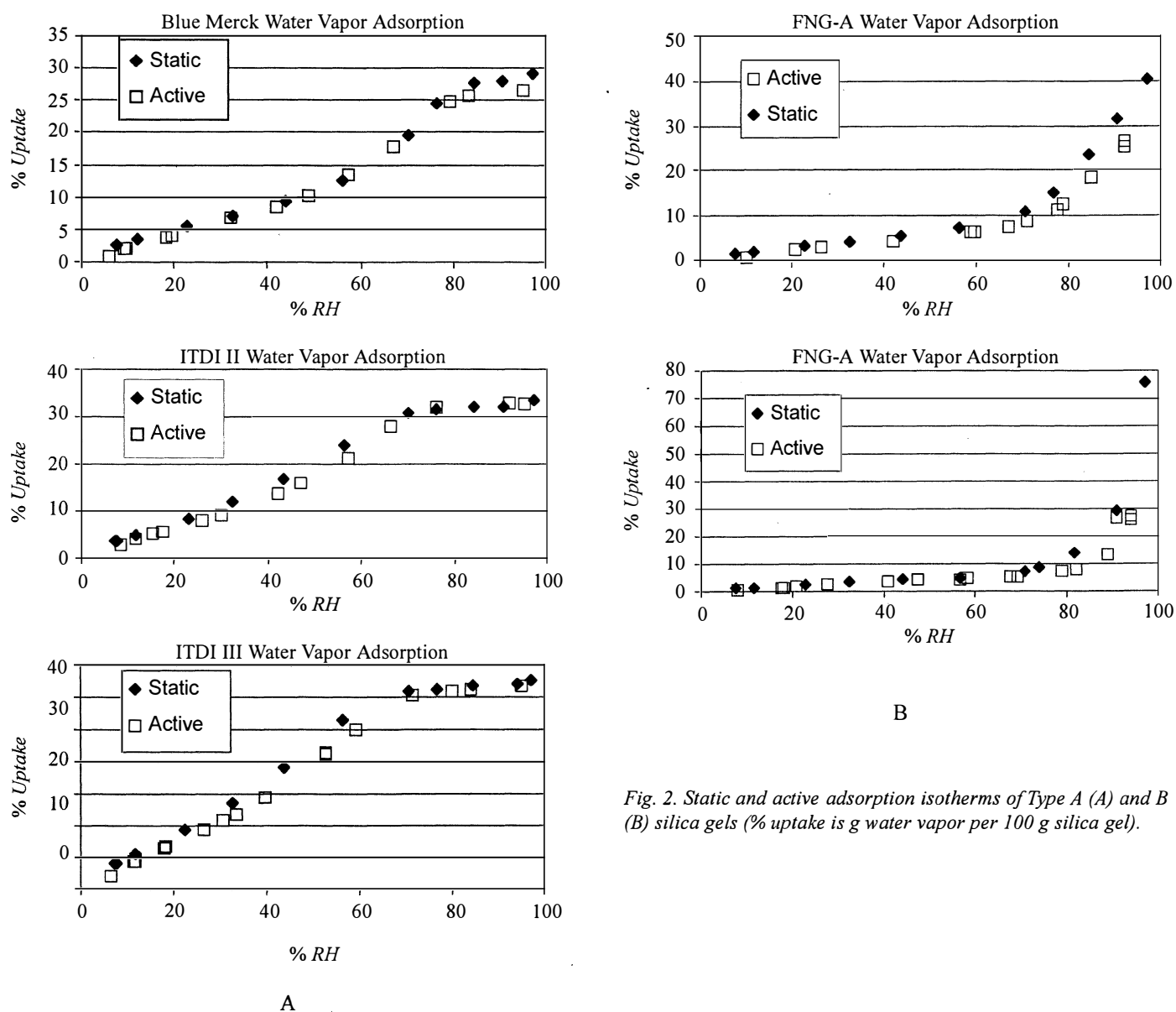


Fig. 2. Static and active adsorption isotherms of Type A (A) and B (B) silica gels (% uptake is g water vapor per 100 g silica gel).

Table 3. BET surface area and $\Delta H_{\text{monolayer}}$ values

| Sample | % RH Range (r)** | | Surface Area* ¹ (m ² g ⁻¹) | | Surface Area* ² (m ² g ⁻¹) | | $\Delta H_{\text{monolayer}}$ (kJ mol ⁻¹) | |
|------------|---------------------|---------------------|--|--------|--|--------|---|--------|
| | Static | Active | Static | Active | Static | Active | Static | Active |
| RHSG 2 | 7.7–22.9 (.998) | 8–18 (.996) | 188.1 | 140.7 | 322.9 | 241.6 | -47.95 | -47.41 |
| FNG-A | 7.7–22.9 (.977) | 20.7–59.6 (.997) | 163.7 | 126.3 | 281.1 | 216.8 | -48.97 | -49.14 |
| ITDI III | 7.4–22.5 (.996) | 11.6–18.2 (.988) | 467.9 | 918.8 | 803.5 | 1577.8 | -48.46 | -46.09 |
| ITDI II | 7.2–22.9 (.995) | 8.6–17.4 (.978) | 451.1 | 601.5 | 774.7 | 1032.9 | -48.28 | -46.82 |
| Blue Merck | 7.2–22.9 (1.000) | 9.8–19.4 (.987) | 269.2 | 545.7 | 462.2 | 937.1 | -48.76 | -46.16 |

*¹ Calculated using 0.11 nm² as effective molecular area of water; *² Calculated using 0.20 nm² as effective molecular area of water; **r is regression correlation coefficient

from 0.7 to 1.5 RH units. The LiCl saturated solution had a 0.7 RH difference during the earlier samples, which enlarged to 1.5 RH units in the equilibration of later silica gel samples. Since values using the same hygrometers compared favorably with values calculated from literature (for the other saturated salt solutions), it is probable that the condition (and/or changes in the condition) of the particular salt solution is responsible for large experimental vs. calculated RH difference. Comparison for the K₂SO₄ saturated solution could not be done because its calculated RH value of 97.1% exceeded the hygrometer range maximum of 94% RH.

Comparison of static and dynamic adsorption isotherms.

Figures 2 (A and B) compare static and dynamic adsorption isotherms for the five silica gel samples. Blue Merck, ITDI II and ITDI III show type A adsorption behavior, characterized by an appreciable water vapor uptake at low to medium RH's followed by a leveling out at near saturation RH values [1]. For ITDI II and ITDI III, active uptake values are lower than static values in the low to intermediate RH regions, and attain comparable values in the higher RH regions where uptake levels out. Blue Merck had comparable dynamic vs. static uptake values in the intermediate RH regions, but had lower active uptake values in both low and near saturation RH regions.

FNG-A and RHSG 2 exhibited type B isotherm behavior, characterized by low uptake at low to intermediate RH regions and progressively increasing uptake in the near saturation RH region [1]. At higher RH's, the dynamic type B isotherms are seen to deviate negatively from the static to a greater extent compared to type A isotherms. The dynamic isotherm setup could not record values beyond 95% RH due to the range limitation of the hygrometers used. From the trends shown in Figure 2B, it is possible that beyond the hygrometer range, the deviation between static and dynamic uptake could progressively increase.

BET (Brunauer, Emmet and Teller) modeling of adsorption data. BET (Brunauer, Emmet and Teller) models adsorption

in a monolayer at low pressures and multilayer formation at higher pressures of the adsorbate. Mathematical treatment of the BET model leads to the equation [6]:

$$[\text{RH}/(1-\text{RH})][1/a] = 1/[(18 N_m)C] + [(C-1)/C][1/(18 N_m)][\text{RH}]$$

where 18 N_m is the amount (in g) of water vapor that forms a monolayer adsorbed on the surface of 1 g of silica gel and a is uptake in g water vapor per g silica gel.

A plot of [1/a][RH/(1 - RH)] vs. RH enables the calculation of C and (18 N_m). From C, ΔH_1° (the heat of adsorption during monolayer formation) can be calculated. The formula for calculating " H_1° " is:

$$\Delta H_1^\circ = -\Delta H^\circ - RT \ln C$$

where ΔH° is the heat of vaporization of water [6].

Table 3 shows the results of fitting the adsorption data to the BET adsorption model. The resulting parameters (18 N_m and C) were used to calculate surface areas and heats of monolayer adsorption for the silica gel samples. The surface area is calculated by multiplying 18 N_m by [(molecular area of water N)/18gmol⁻¹], where N is the Avogadro Number (number of molecules in a mole of substance). The monolayer of water is not well-defined, causing differences in literature values for the effective molecular area of water. Two values were used [7] as shown in Table 3: the area of an isolated water molecule (0.11 nm²) and an effective molecular area due to clustering (0.20 nm²). The latter value is postulated [7] based on hydrogen bonding between water vapor and silica gel, resulting in the clustering of water molecules around favorable sites. The surface areas from the static isotherms, using the 0.20 nm² value, were most similar to the 200–800 m²g⁻¹ range of static BET surface areas of commercial silica gels found in literature [8]. These commercial values were calculated from nitrogen gas isotherms determined at very low (liquid nitrogen) temperatures

using expensive commercial instruments. Dynamic surface areas were lower than static values for the Type B samples (dynamic to static ratios of 0.75–0.77). The opposite is true for the Type A samples, where dynamic surface areas were significantly higher than static values (dynamic to static ratios of 1.33–2.02).

Monolayer heats of adsorption values were generally lower when calculated from the dynamic, compared to the static, isotherm data (except for FNG-A). The static/dynamic differences, however, were small (0.2–0.5 kJ mol⁻¹) for the Type B samples, compared to the larger differences (1.5–2.6 kJ mol⁻¹) for the Type A samples.

DA (Dubinin-Astakhov) modeling of adsorption data. The BET multilayer adsorption model is based on interaction of a gas molecule with other adsorbed gas molecules, and is equivalent to liquefaction of the gas. For solids with small pores, the adsorbate experiences enhanced attractive forces from the pore walls, causing filling up of the pores with condensed adsorbate at pressures below the saturated vapor pressure of the adsorbate. The phenomenon is modeled by Dubinin-Astakhov (DA) as

$$W = W^* \exp [-(A/E)^n]$$

where A is the adsorption potential (the difference in free energy between the adsorbed phase and the saturated liquid) and E is the characteristic energy of adsorption [1]. W is the volume of the micropore filled by the adsorbate and W* is the micropore volume filled at the saturation pressure. Since W and W* are proportional to uptake (a), we get:

$$a = a^* \exp [-(A/E)^n]$$

where a* is the uptake at 100% RH. A can be calculated from:

$$A = -RT \ln (P/P^0)$$

and n = 1, 2 or 3, each value respectively corresponding to adsorption on the surface, in micropores and in ultramicropores. These values are due to the adsorbed molecules losing one, two or three degrees of freedom. P⁰ is the saturation pressure of the adsorbate. Plotting ln A vs. (A)ⁿ gives a straight line, from which E and a* can be calculated. Later DA models also allowed for n values between 1 and 3 which are not whole numbers.

Table 4 shows the results of DA modeling of the adsorption data. Type B values fitted best for n = 1, while Type A data (except for Blue Merck) fitted best for n = 2. A value near 2 (n = 1.7) was used for Blue Merck.

Two linear RH regions were found for all samples. The lower RH region had bigger characteristic energies of adsorption (E's) compared to the near saturation RH region. The difference is significantly larger for the Type B, compared to the type A samples. The magnitude of E is positively correlated to the strength of adsorbent-adsorbate interactions. For both RH regions, E's of the Type A samples were larger than the Type B's, indicative of stronger water vapor—silica gel interactions (i.e., smaller pores) for the Type A samples. In general, for all samples, except Blue Merck) static E's were higher than dynamic E's. The static/dynamic E difference, however, was small for Blue Merck.

Static/dynamic differences in saturation uptake were very small for the Type A samples but significant for the Type B's. This was expected from the shapes of the experimental adsorption isotherms (Figs. 2 A and B) and indicates the good fit of the DA model for both low and high RH regions.

Isosteric heats of adsorption. Assuming that the adsorption process of water vapor on silica gel is a phase transition process analogous to condensation, the Clausius Clapeyron equation

Table 4. Dubinin-Astakhov (DA) values for E (Characteristic Energy of Adsorption) and a* (Saturation Uptake)

| Sample | %RH Range (r)** | | E (kJmol ⁻¹) | | a* (g water/g silica gel) | |
|------------|-----------------|-------------------|--------------------------|--------|---------------------------|--------|
| | Static | Active | Static | Active | Static | Active |
| RHSG 2 | 7.4–43.5 (.998) | 8.0–69 (.998) | 3.41 | 2.88 | .726 | .57 |
| | 76.1–97 (.995) | 88.9–94.1 (.9999) | .37 | .21 | | |
| FNG-A | 7.8–43.7 (.996) | 20.7–67.1 (.996) | 3.72 | 2.66 | .47 | .381 |
| | 70.5–97 (.999) | 77.7–92.3 (.997) | .60 | .54 | | |
| ITDI III | 7.4–22.5 (.994) | 6.4–32.6 (.996) | 5.94 | 4.99 | .33 | .323 |
| | 32.6–97 (.997) | 39.4–95.3 (.997) | 2.95 | 2.59 | | |
| ITDI II | 7.2–22.9 (.994) | 8.6–30 (.995) | 5.86 | 5.00 | .336 | .334 |
| | 43.5–97 (.996) | 42–95 (.993) | 2.54 | 2.27 | | |
| Blue Merck | 7.8–32.6 (.997) | 6.3–48.7 (.989) | 5.35 | 3.97 | .299 | .282 |
| | 56.4–97 (.995) | 57.5–95.3 (.992) | 1.55 | 1.64 | | |

**r is regression correlation coefficient

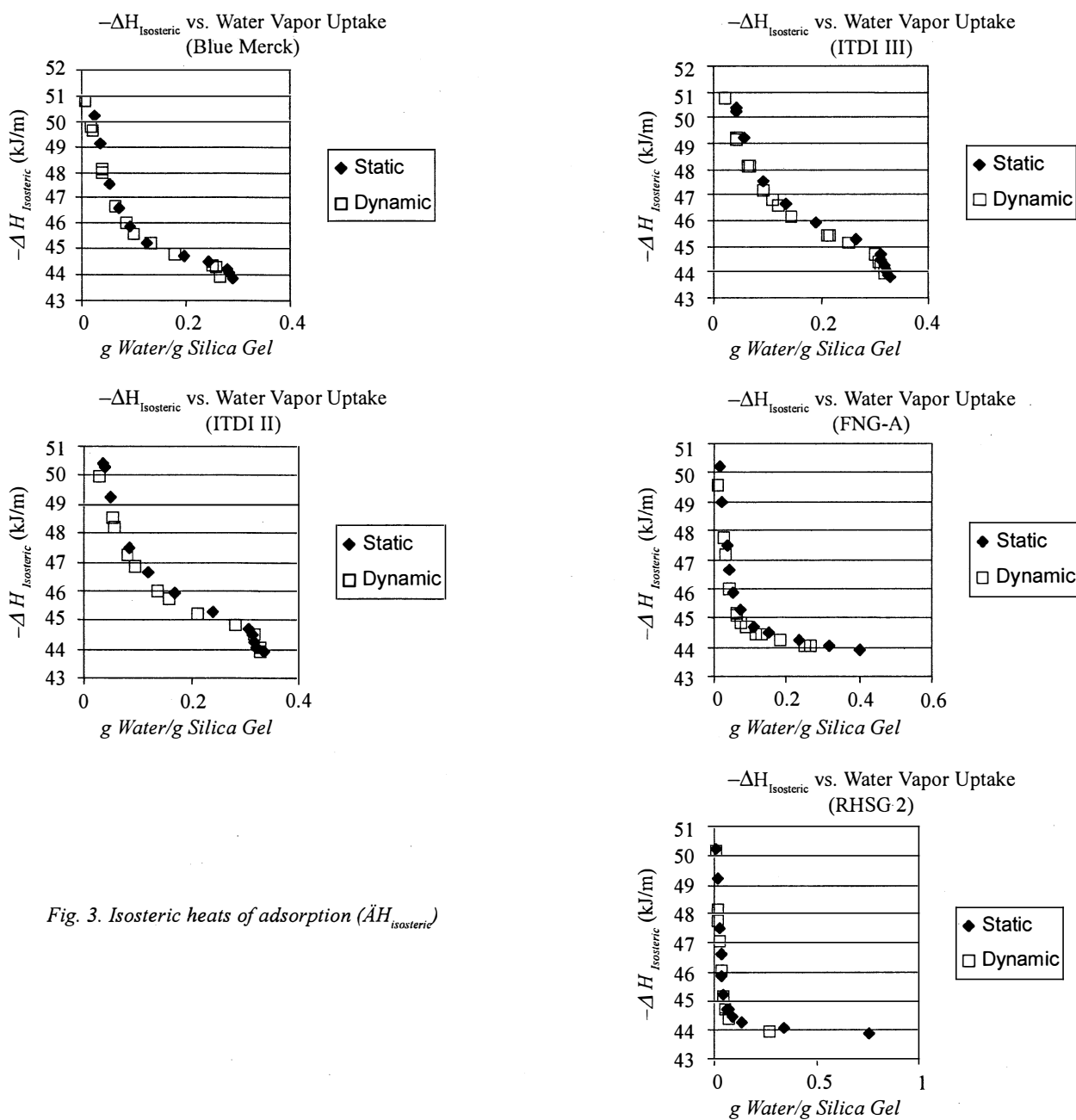


Fig. 3. Isosteric heats of adsorption ($\Delta H_{\text{isosteric}}$)

[9] can be combined with the DA equation to calculate $\Delta H_{\text{isosteric}}$ (heats of adsorption at different water vapor uptake values). The final derived formula [3] is

$$\Delta H_{\text{isosteric}} = -A - R b T^2 / (T + c)^2$$

The absolute value of the second term on the right side of the equation is the heat of vaporization of water. Therefore, $\Delta H_{\text{isosteric}}$ is the negative sum of A (the adsorption potential energy) and the heat of vaporization of water [3].

Figure 3 shows the calculated $\Delta H_{\text{isosteric}}$ values plotted vs. water vapor uptake. Static and dynamic values are close even for the near saturation RH regions of the Type B's, in spite of significant

differences in uptake. Type A samples release significantly greater amounts of heat during the adsorption process compared to Type B samples, as seen from the areas under the plots of the two types. For both types, heats of adsorption at near saturation RH's approach the value of the heat of condensation of water (approximately -44 kJmol^{-1}).

CONCLUSION

Static and dynamic adsorption isotherms of water vapor on various silica gel samples were found to have similar shapes (for each sample). For the type A samples, ITDI II and III had close static/dynamic adsorption uptake values at high RH's,

while Blue Merck had similar static/dynamic adsorption uptake values in the intermediate RH regions. In the other regions, the dynamic uptake values were generally lower than the static values. The dynamic isotherms of the type B gels FNG-A and RHSG 2 deviated negatively from the static to a greater extent compared to the type A deviations at higher, near saturation RH's. This could be due to limitations in the dynamic process such as incomplete attainment of saturation (complicated by range limitations of the hygrometers used) and heat transfer effects.

The heat transfer effects, however, would be more likely at low to intermediate RH's for the Type A samples, as seen in the heats of adsorption released (Fig. 3). In the static process, the sorption process (and the accompanying heat production) is considerably slower and the space for heat dispersion much greater compared to the dynamic set-up. This leads to a greater possibility of non-isothermal conditions occurring during the dynamic adsorption process.

As a whole, in spite of static and dynamic differences in values calculated from BET and DA model parameters, general conclusions as to the structure of the silica gels (i.e., smaller pores and/or stronger sorbate-sorbent interactions for the type A samples compared to the type B's) were the same, as seen in heats and energies of adsorption calculated from both static and dynamic results.

Heats of adsorption were better modeled by the DA, compared to the BET, equation. Heats of adsorption were comparable for the two silica gel types in terms of BET monolayer values, but were clearly seen in DA derived isosteric heats of adsorption and characteristic adsorption energies, to be significantly larger for the type A samples. This was due to the larger range of RH applicability (from low to near saturation regions) for the DA equation. The BET equation was useful only for parameters at monolayer coverage (low RH region).

Surface areas, however, are derived using the monolayer values of the BET model, and this is where static and dynamic differences are most significant. This is especially true for the type A samples, whose dynamic surface area values were 1.3–2.0 times the static values.

The dynamic method is indicated by this study to be useful for fast determination of water vapor-silica gel adsorption isotherms, except for near saturation regions for type B gels. Extraction of thermodynamic and physical parameters from the isotherms by mathematical modeling yielded better fits (based on regression correlation coefficients) and more reasonable surface area values (based on literature) for the equilibrium method.

ACKNOWLEDGMENT

The authors are grateful to the Department of Agriculture Bureau of Agricultural Research (DA-BAR) for funding this research, to University of the Philippines-Natural Sciences Research Institute (UP-NSRI) for providing the research facilities for this study and to Nanda Suavillo of CMD ITDI for the ITDI samples.

REFERENCES

1. Suzuki, M. *Adsorption Engineering*, p. 5. (Elsevier, 1990).
2. Tsami, E., Marinos-Kouris, D., and Maroulis, Z. B. *J. Food Sci.* 55 (6), 1594 (1990).
3. Park, I. and Knaebel, K. S. *AIChE Journal*. 34 (5), 660 (1992).
4. Suavillo, E. A., Paramil, Y. S., and Zalameda, M. D. *Phil. J. Sci.* 120 (3), 329 (1991).
5. Wexler, A. *Handbook of Chemistry and Physics*, 76th Ed., p. 15. (1997).
6. Castellan, G. W. *Physical Chemistry*, 3rd ed., p. 428. (Addison Wesley Publishing Co., 1983).
7. Gregg, S. J. and Sing, K. S. W. *Adsorption, Surface Area and Porosity*. (Academic, 1982).
8. Scott, R. P. W. *Silica Gel and Bonded Phases*, p. 5. (John Wiley & Sons Ltd., 1993).
9. Atkins, P. W. *Physical Chemistry*, 6th ed., p. 152. (Oxford University Press, 1998).